The influence of heteroatoms substitution in cross-conjugation and their effect on the photovoltaic performance of DSSCs - A computational investigation on linear vs. cross-conjugated anchoring units

Mahalingavelar Paramasivam[†,], Ramesh kumar Chitumalla[‡], Joonkyung Jang[‡] and Ji Ho Youk[†]*

[†] *Department of Applied Organic Materials Engineering, Inha University, Incheon 22212, Republic of Korea.*

[‡] *Department of Nanoenergy Engineering, Pusan National University, Busan 46241, Republic of Korea*

Table of contents

Theoretical methods

The most influential parameters in determining the PCE (η) of DSSC are short-circuit current density (J$_{sc}$), open-circuit photo voltage (V$_{oc}$), and fill factor (FF). Among them J$_{sc}$ and V$_{oc}$ can be tuned by the appropriate substitution of π-building blocks. J$_{sc}$ is directly proportional to the light harvesting efficiency (LHE) and electron injection efficiency (Φ_{inject}) of the dyes that can be calculated from the DFT computed parameters such as oscillator strength (f) and electron injection driving force (ΔG^{inject}) respectively. The short-circuit current density can be described in the integral form as

$$J_{sc} = e \int_{\lambda} LHE(\lambda)\Phi_{inj}\eta_{reg}\eta_{coll}I_s(\lambda)d\lambda \tag{1}$$

Where, η_{reg}-electron regeneration efficiency and η_{coll}-electron collection efficiency. The light harvesting efficiency of the dyes could be obtained at their maximum absorption according to the formula:

$$LHE = 1 - 10^{-f} \tag{2}$$

Where, f-oscillator strength of the maximum absorption obtained at longer wavelength that depends on the overlap between initial and final state wave functions upon photoexcitation. To evaluate the electron injection efficiency, it is appropriate to calculate the closely related exciton binding energy (E_b) and driving force for electron injection (ΔG^{inject}). This value has been extracted from the excited state oxidation state potential state of the dyes@TiO$_2$. These both values can be calculated through the following expression:

$$\Delta G^{inject} = E^{dye*} - E_{CB} \tag{3}$$

$$E^{dye*} = E^{dye} - E_{0-0} \tag{4}$$

Where, E_{CB}- conduction band of the $(TiO_2)_{16}$ semiconductor and the value of -3.97 eV has been used in this study. E^{dye}- ground state oxidation potential; E_{0-0}- vertical excitation energy. The relative binding strength of the dyes upon TiO$_2$ adsorption is defined as:

$$E_{Ads} = E_{dye@TiO_2} - [E_{dye} + E_{TiO_2}] \tag{5}$$

Where, $E_{dye@TiO_2}$ – energy of the dye after adsorption on $(TiO_2)_{16}$; E_{dye}- energy of the isolated dye; E_{TiO_2}-energy of the bare $(TiO_2)_{16}$ cluster. The rate of electron injection from dye to TiO$_2$ semiconductor is measured based on the electronic coupling strength and energetic shift of LUMO (ads). For the purpose, Newns-Anderson model has been adopted to describe the change in molecular orbital levels of the dyes upon TiO$_2$ adsorption. The centre of LUMO(ads) distribution obtained from the portions (p_i) of the orbital located on the dyes is written as.

$$E_{LUMO}(ads) = \sum_i p_i \varepsilon_i \tag{6}$$

The LUMO broadening is obtained from the average deviation of the distribution of the positioned LUMO(ads) that can be evaluated using the relation:

$$\hbar\Gamma = \sum_i p_i \left| \varepsilon_i - E_{LUMO}(ads) \right| \qquad (7)$$

Where, ε_i- orbital energies of the combined system in the selected energy range. Finally, for a better convenience, the electronic coupling strength obtained from LUMO broadening in the order of meV is converted into the direct estimation of electron-transfer time scale using the formula:

$$\tau(fs) = 658/\Gamma(meV) \qquad (8)$$
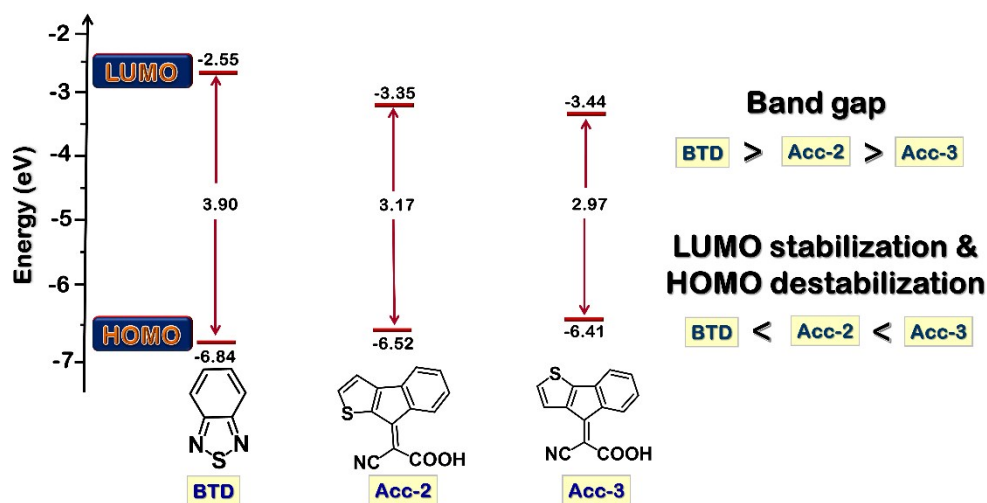

Fig.S1 Energy levels of the bare acceptor units obtained from the B3LYP/6-311g(d,p) level of theory.
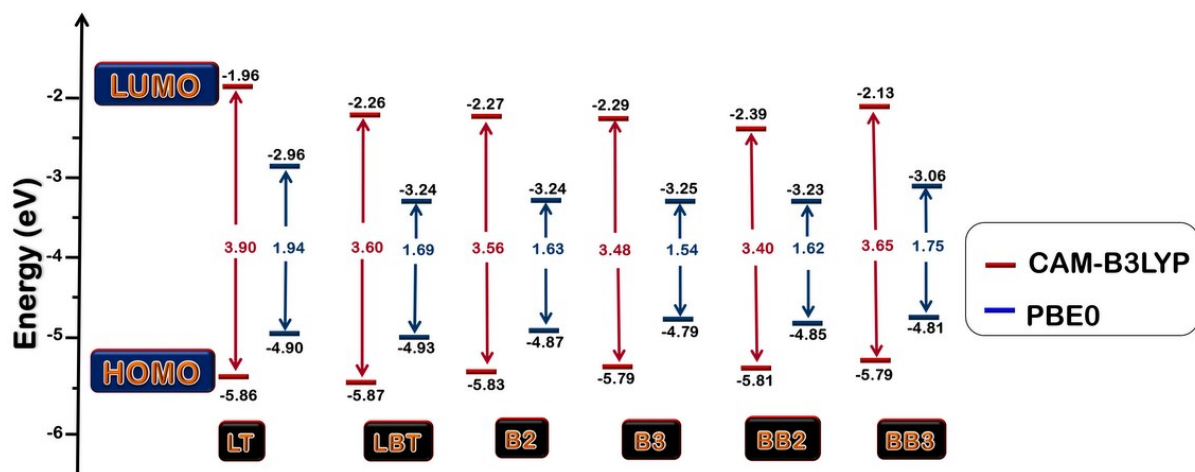
Fig. S2 Energy levels of the dyes obtained from the CAM-B3LYPand PBE1PBE/6-311g(d,p) level of theory.
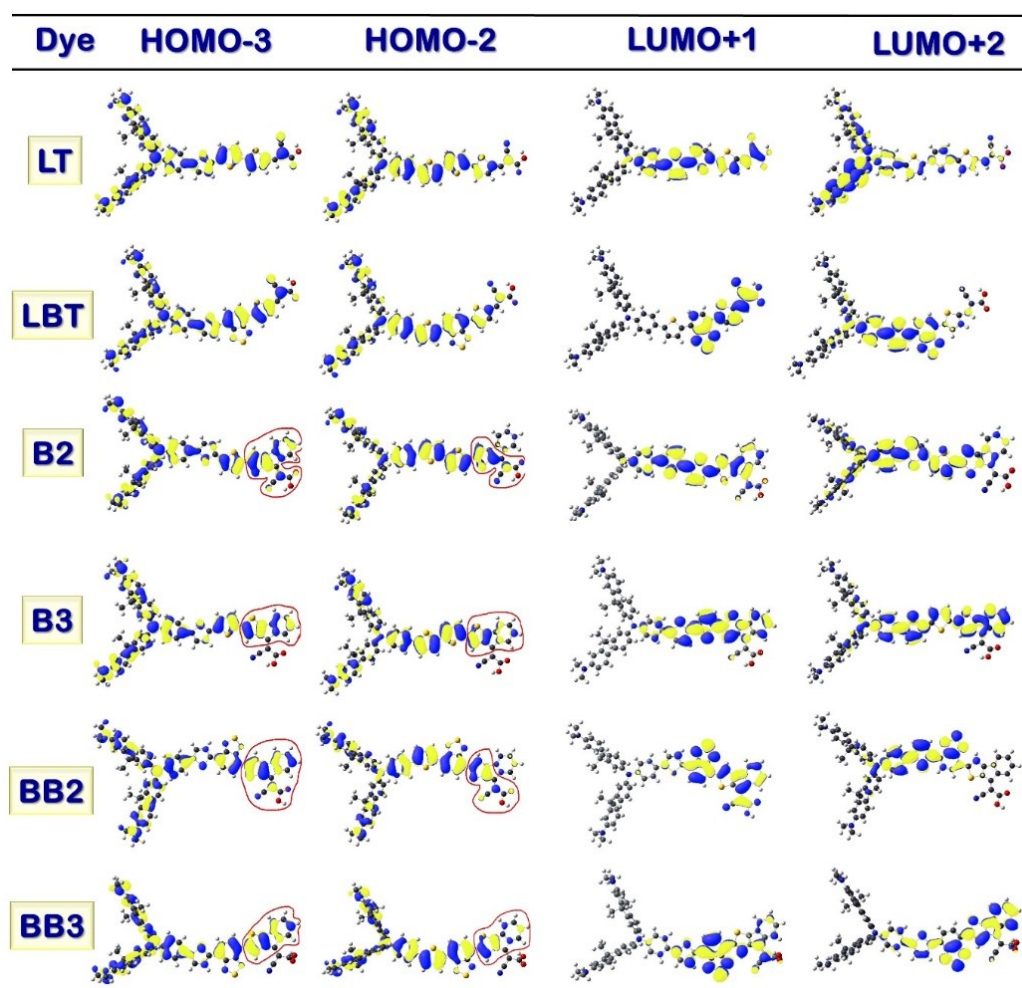
Fig. S3 FMOs of HOMO-3, HOMO-2, LUMO+1 and LUMO+2 of the dyes, which are majorly involved in transitions and the red colour indicates the π-delocalization path.
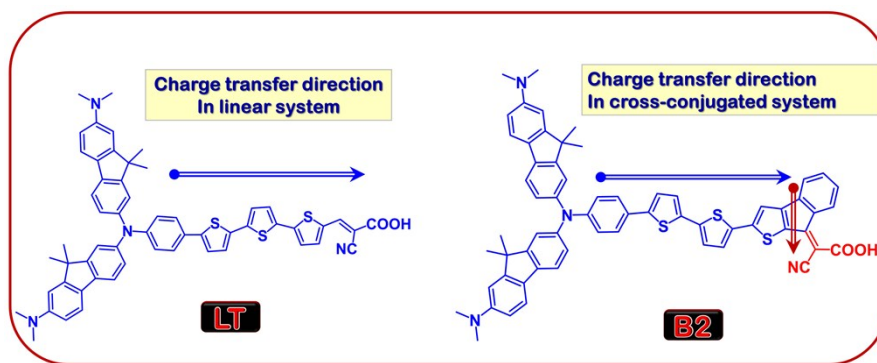
Fig. S4 Charge transfer direction of the linear and cross-conjugated dyes.

S.No	Compound	E_{ox} (V) and HOMO (eV)	E_{red} (V) and LUMO (eV)	bandgap (eV)	Ref
1		1.00 V (-5.87 eV) (-5.25 eV)	-0.80 V (-4.33 eV) (-3.11 eV)	1.80 V (1.54 eV) (2.14 eV)	2
2		0.92 V (-5.79 eV) (-5.10 eV)	-0.83 V (-4.29 eV) (-3.18 eV)	1.75 V (1.50 eV) (1.92 eV)	2
3		1.04 V	-1.02 V	2.06 V	3
4		0.97 V	-0.72 V	1.69 V	3
5		1.44 V (-6.36 eV)	-0.96 V (-3.58 eV)	2.40 V (2.78 eV)	4
6		1.27 V (-6.25 eV)	-0.98 V (-3.60 eV)	2.25 V (2.66 eV)	4
7		1.22 V (-5.75 eV)	-1.06 V (-3.33 eV)	2.28 V (2.43 eV)	5
8		0.85 V (-5.48 eV)	-1.04 V (-3.39 eV)	1.89 V (2.10eV)	5

Fig. S5 Reported electrochemical oxidation, reduction potentials and band gap obtained from cyclic voltammetry technique and their HOMO and LUMO values. (Electrochemical band gap is indicated red in colour; DFT computed HOMO and LUMO values are indicated in blue colour).
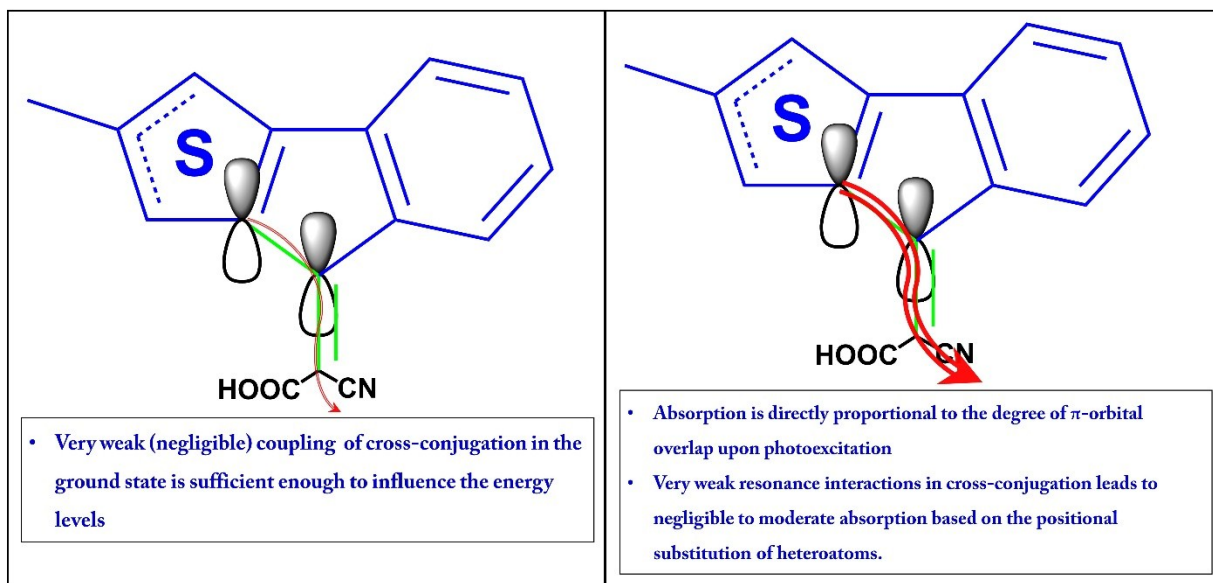
Fig. S6 Schematic representation illustrating the extent of π-orbitals overlap needed to influence the energy levels and photophysical properties.
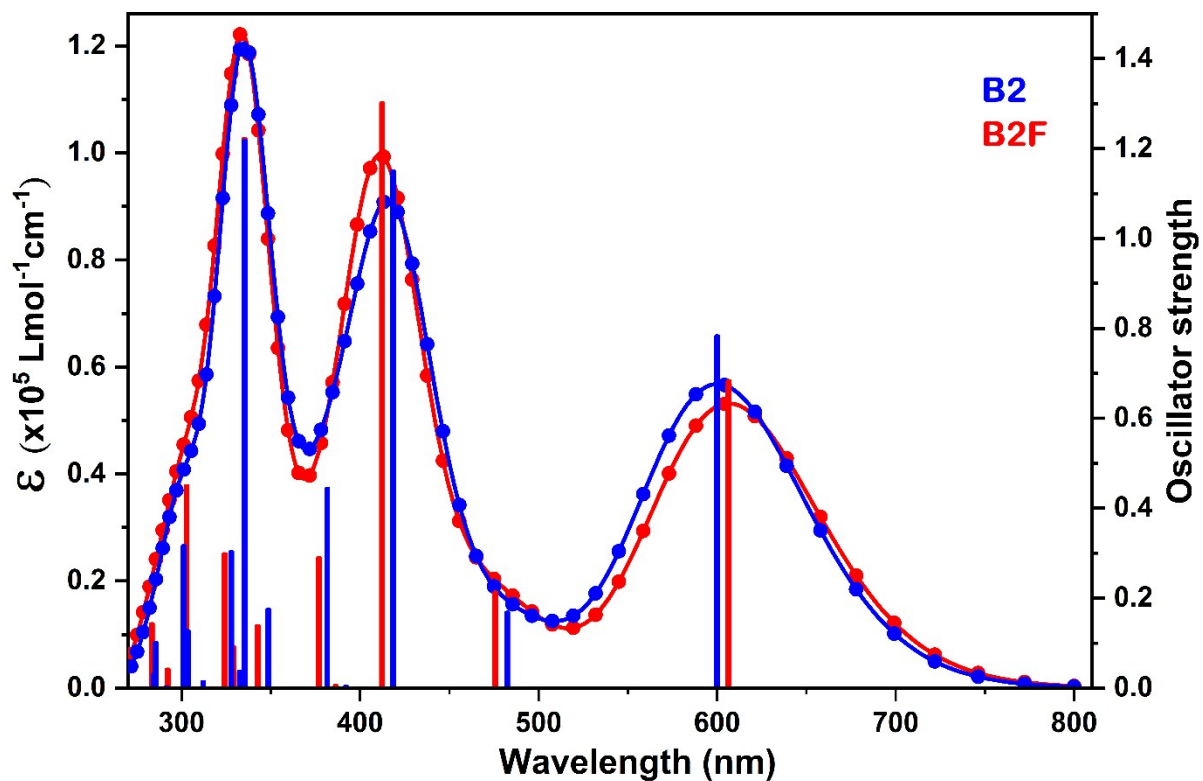
Fig. S7 Comparison of the TDDFT results for B2 and B2F obtained from the M062X/6-311g (d, p)/C-PCM(THF) level of theory.
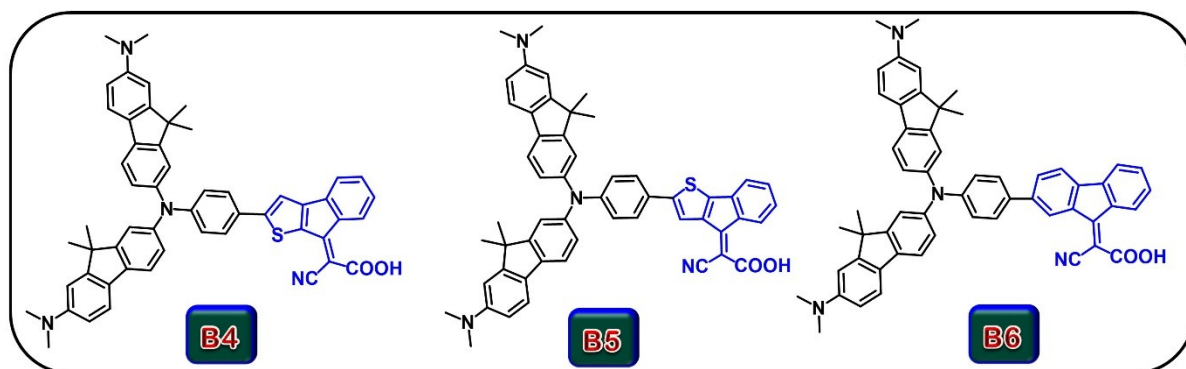
Fig. S8 A series of the bridged dyes have been used to investigate the π-delocalization pathway.
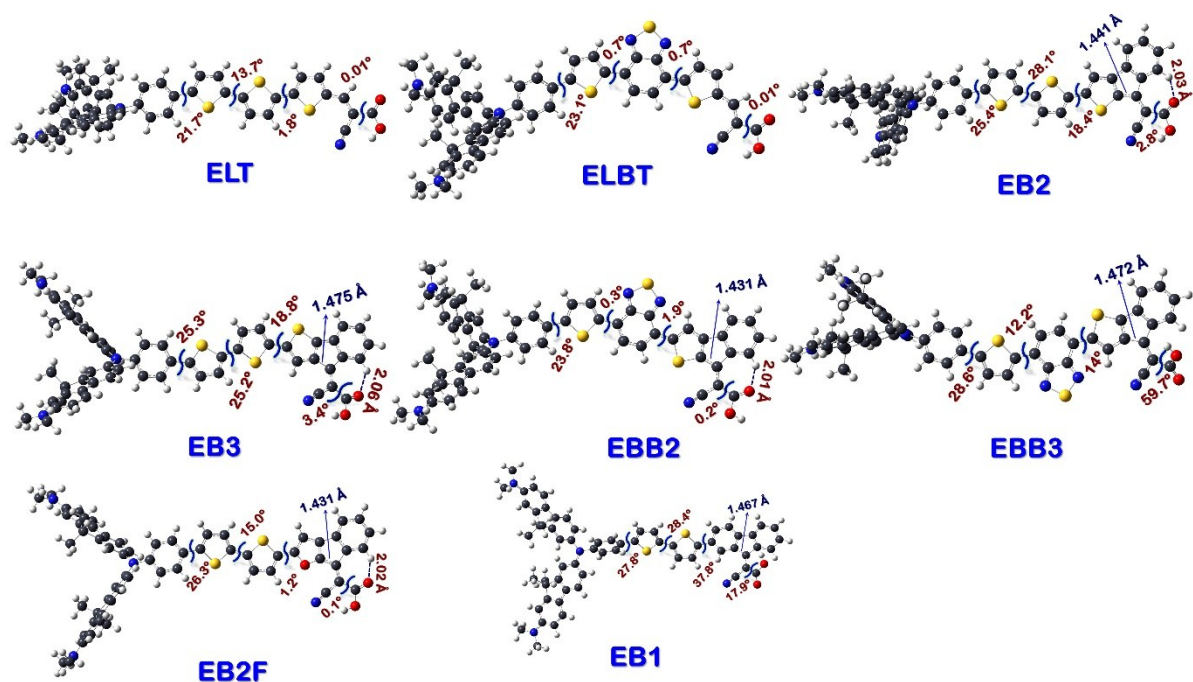
Fig. S9 Excited state geometry of the dyes obtained from TD/B3LYP/6-311g (d, p) level of theory.
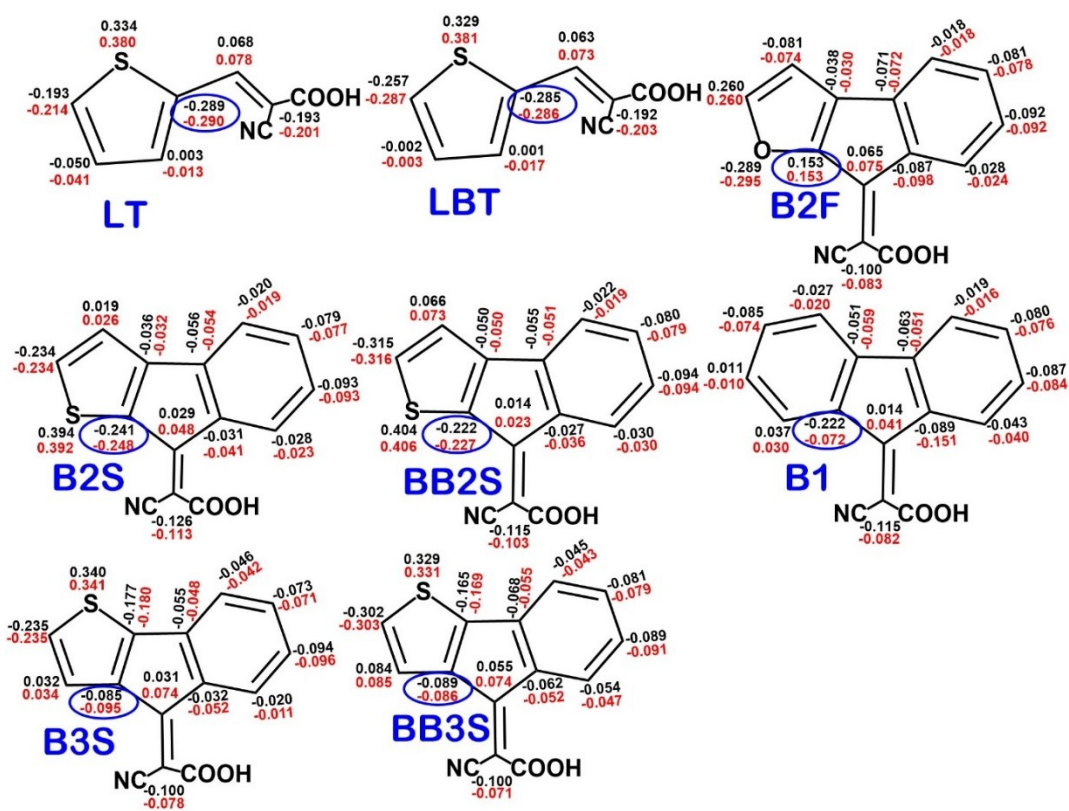
Fig. S10 Mulliken charge population analysis of the dyes in the ground (black) and excited state (red).
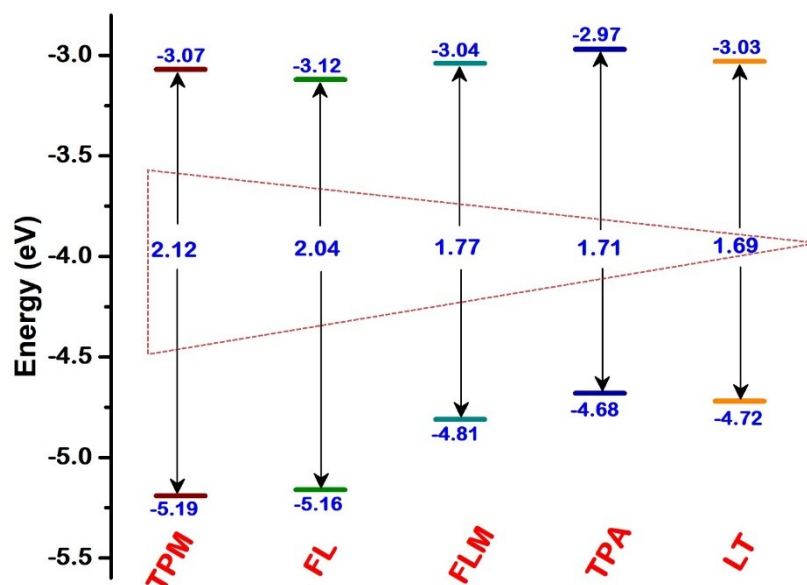
Fig. S11 Evaluation of the donor strength by comparing the energy levels with the previously reported donors.
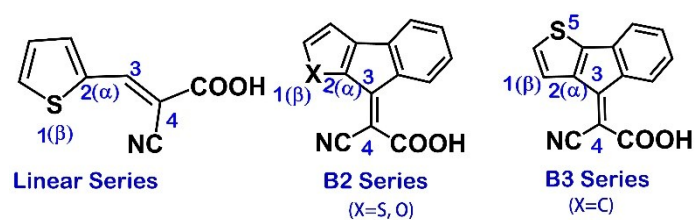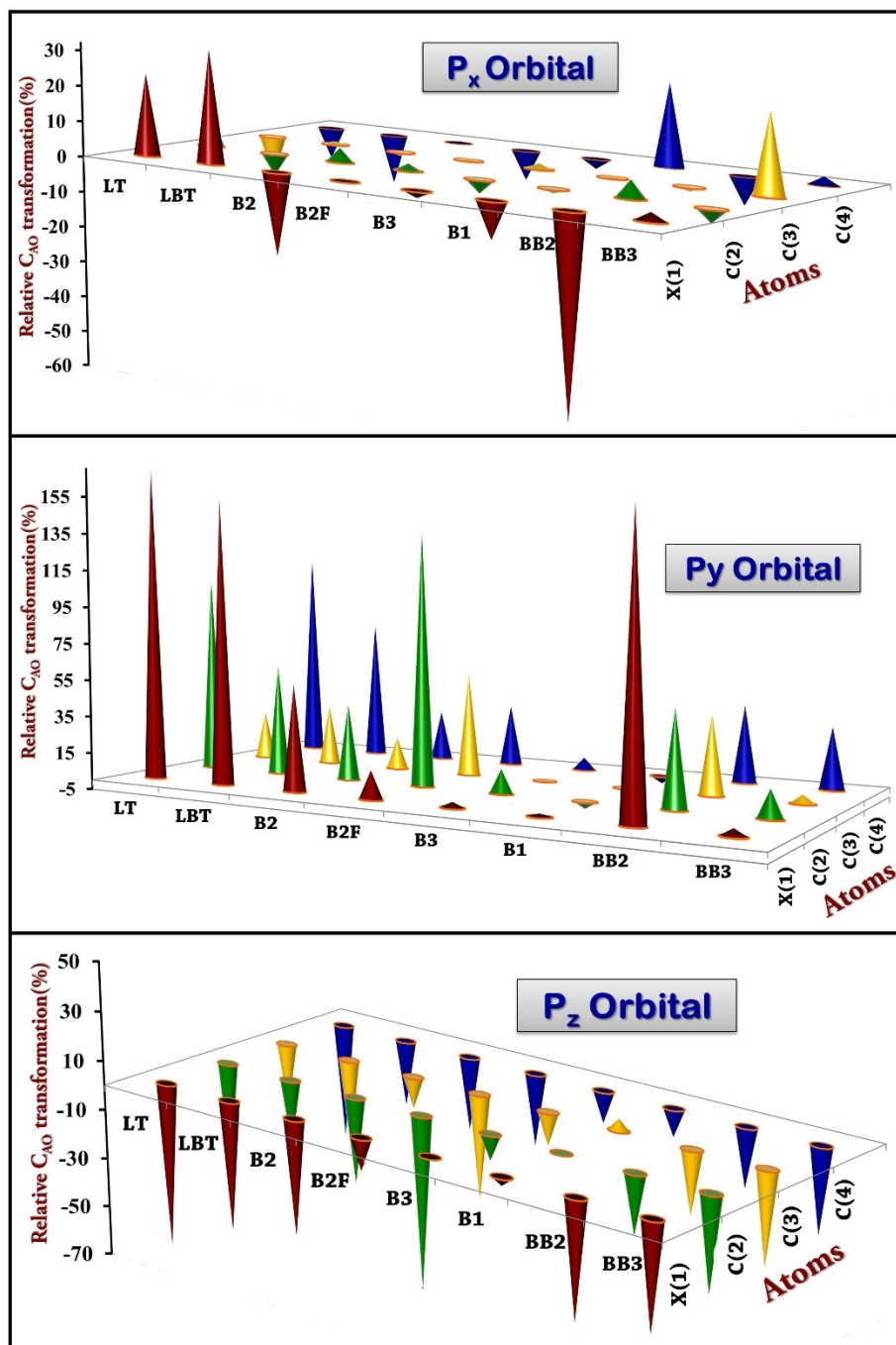
Fig. S12 Relative percentage C_{AO} transformation of X_β-C_α-C_b-C_v from ground to excited state.
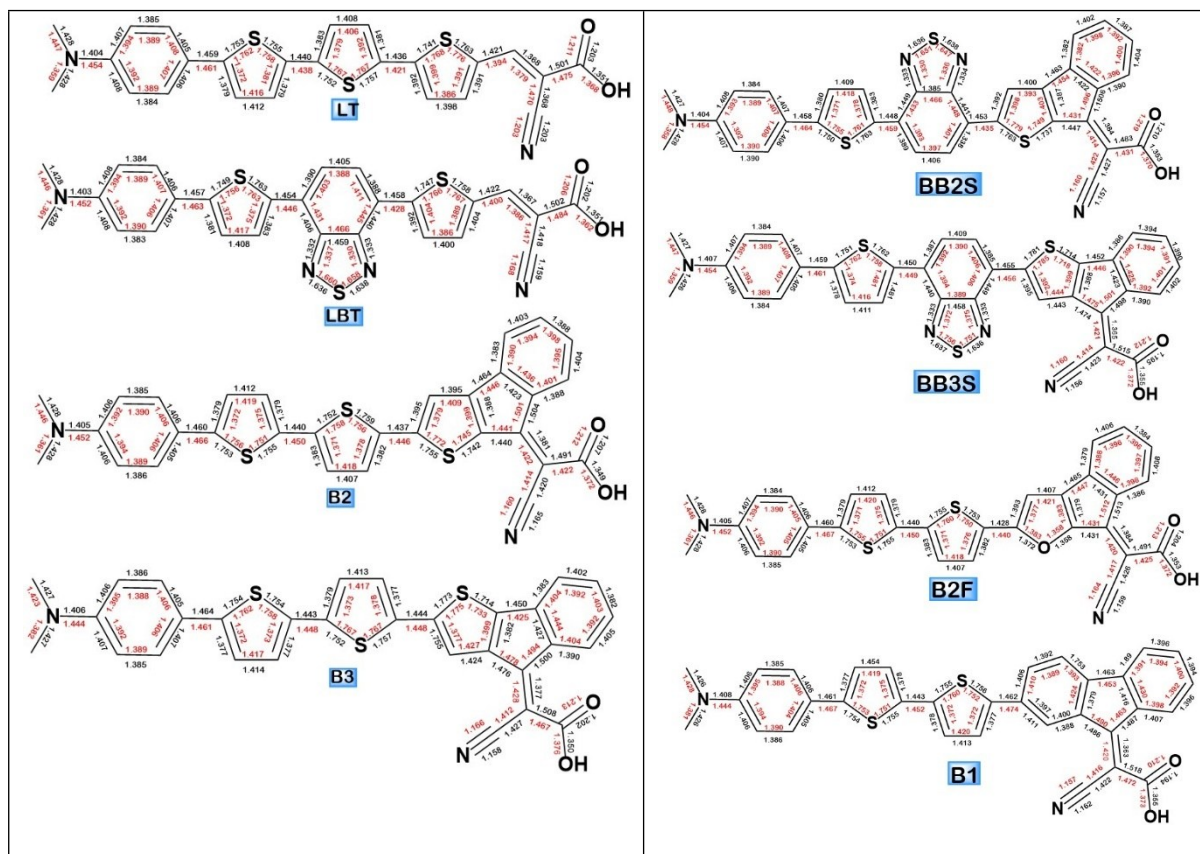
Fig. S13 Geometrical coordinates of the dyes
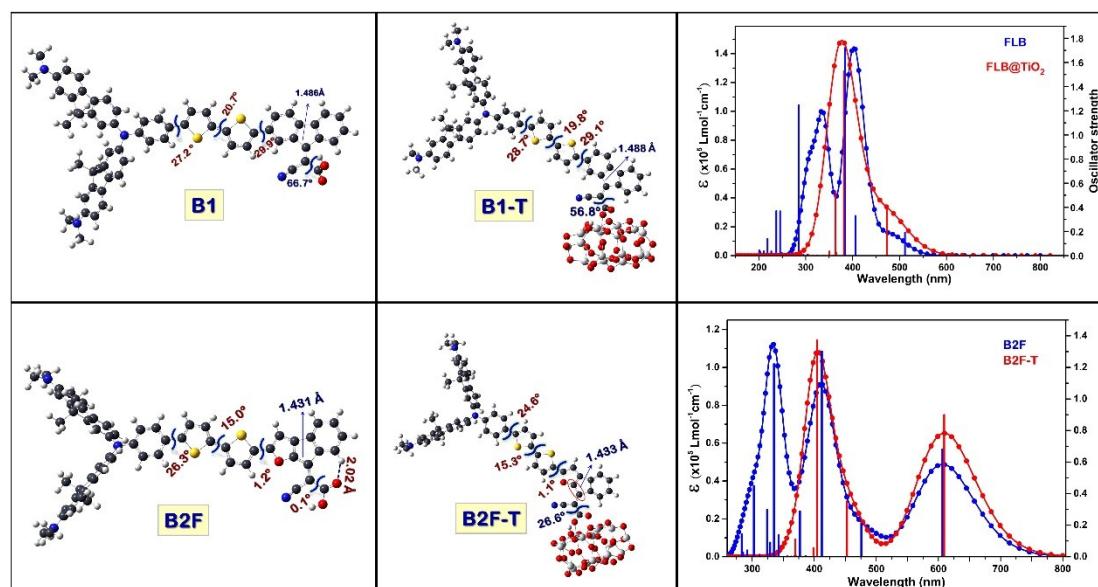
Fig. S14 Optimized geometries of B1, B2F dyes with significant geometrical parameters and TDDFT simulated spectra of the isolated dyes vs. dyes@(TiO$_2$)$_{16}$.
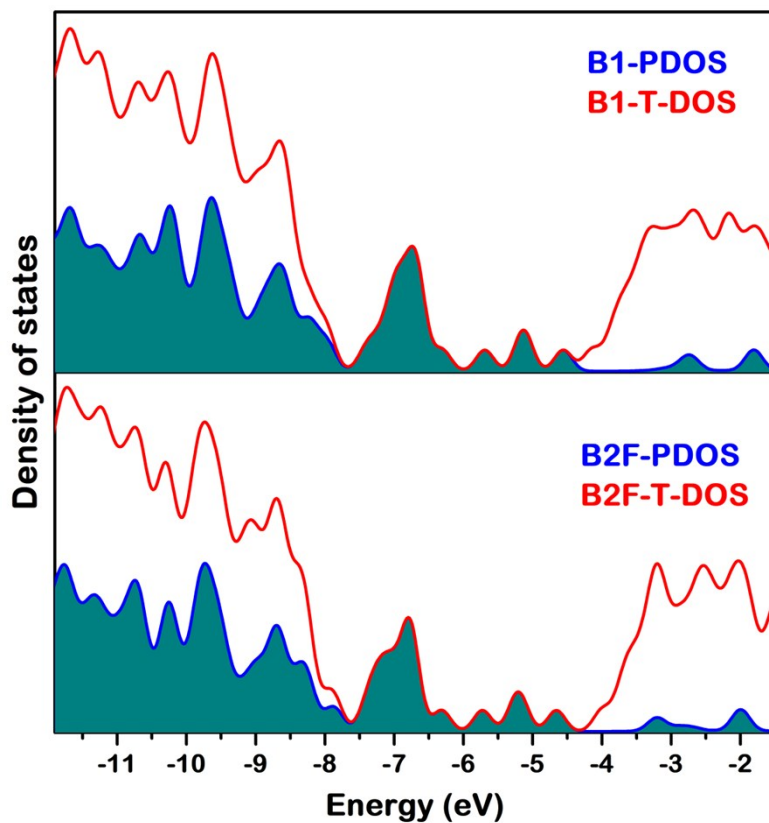
Fig. S15 DOS and PDOS of B2F and B1 dyes@$(TiO_2)_{16}$.
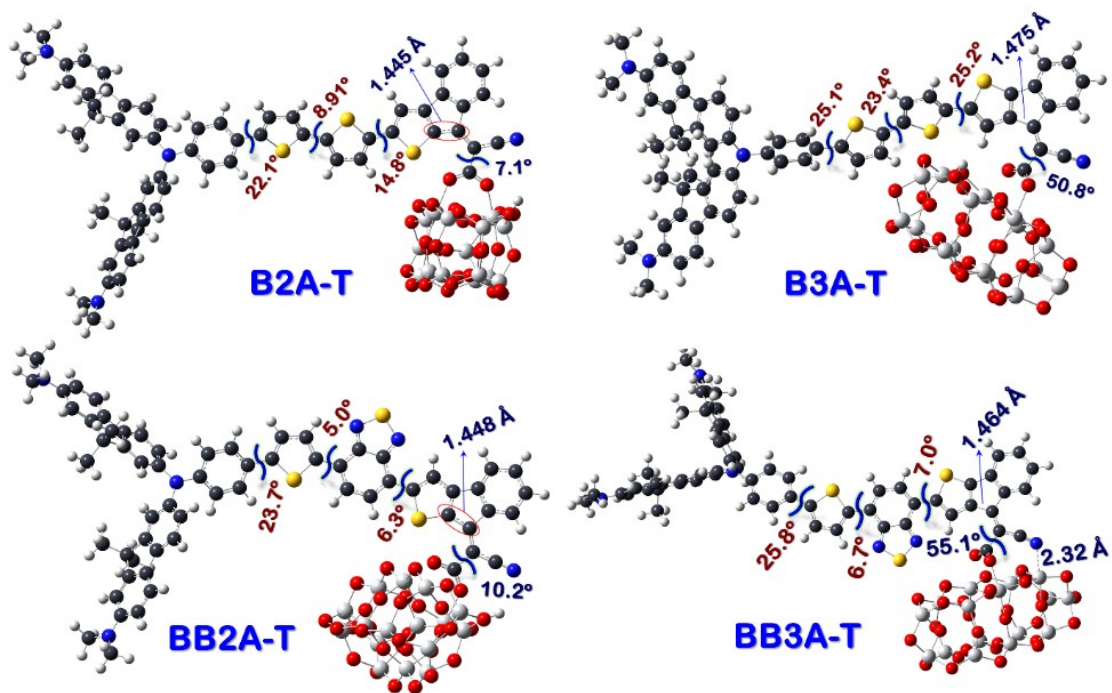
Fig.S16 Optimized geometries of the bridged dyes@TiO_2 with 'A' anchoring mode depicting selected bond distance and dihedral angles.
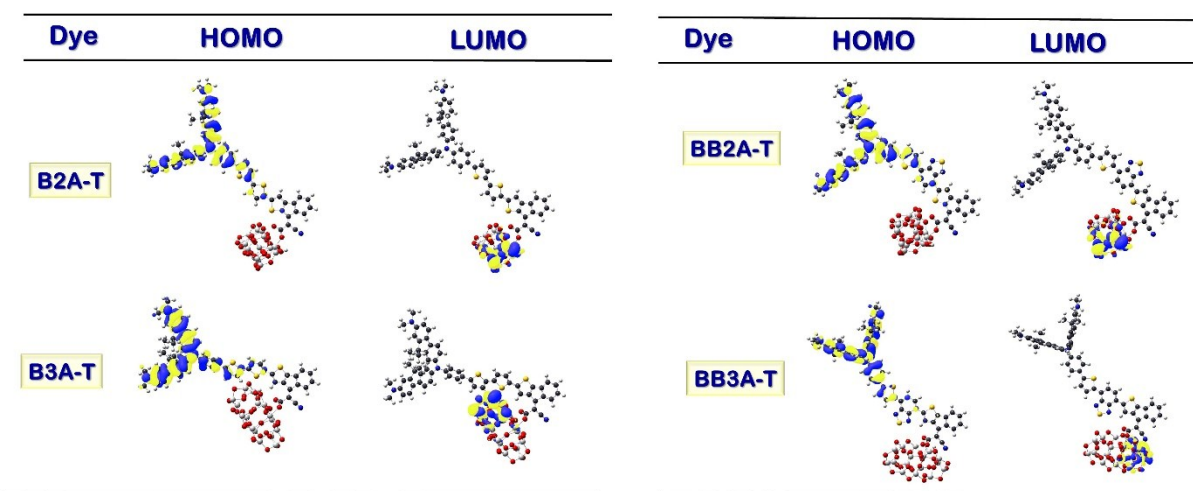
Fig. S17 Isodensity molecular orbital amplitudes of HOMO and LUMO of the bridged dyes@TiO$_2$ with 'A' anchoring mode.
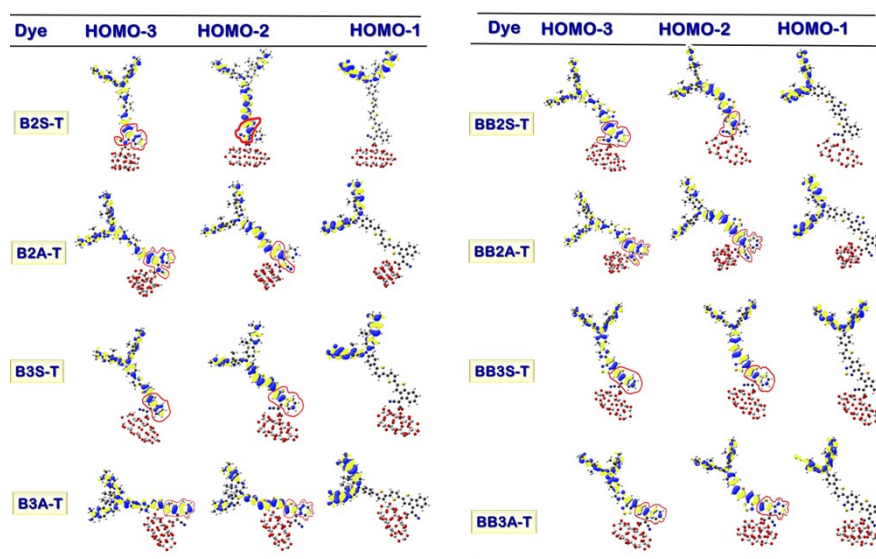
Fig. S18 HOMO-3, HOMO-2, HOMO-1 of the dyes@TiO$_2$ and the red colour indicates the π-delocalization path.
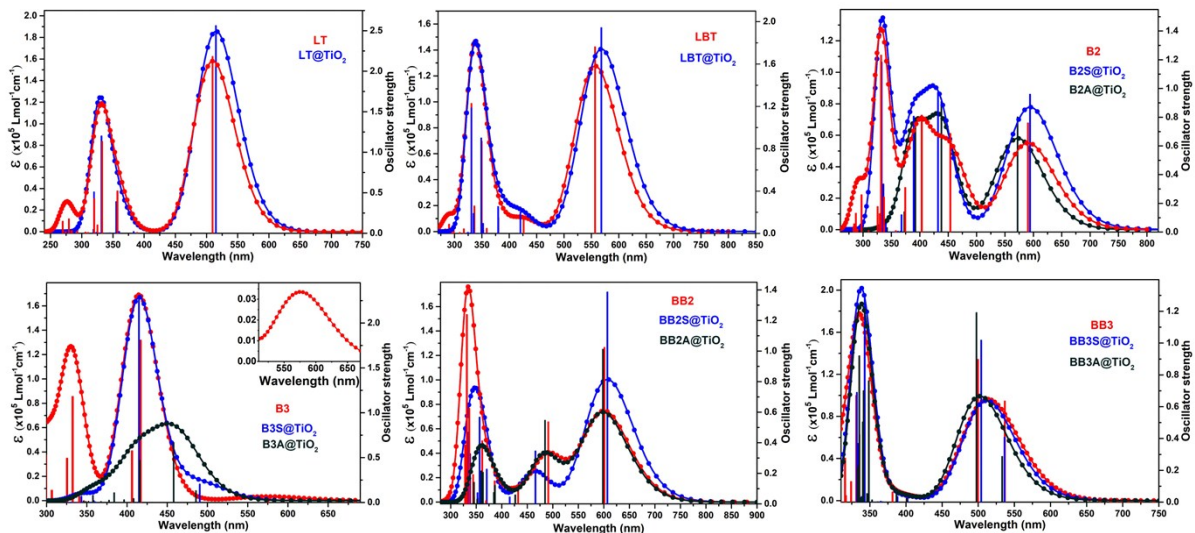
Fig. S19 Comparison of simulated absorption spectra of dyes and dyes@TiO$_2$ obtained from CAM-B3LYP/6-311g(d, p)/C-PCM(THF) level of theory.
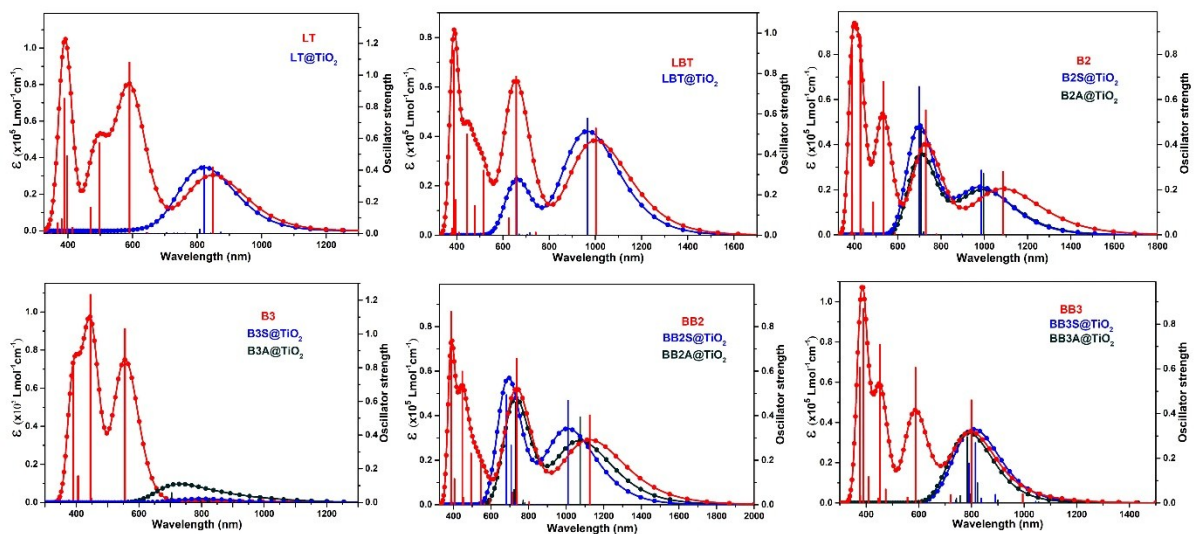
Fig. S20 Comparison of simulated absorption spectra of dyes and dyes@TiO$_2$ obtained from B3LYP/6-311g(d, p)/C-PCM(THF) level of theory.
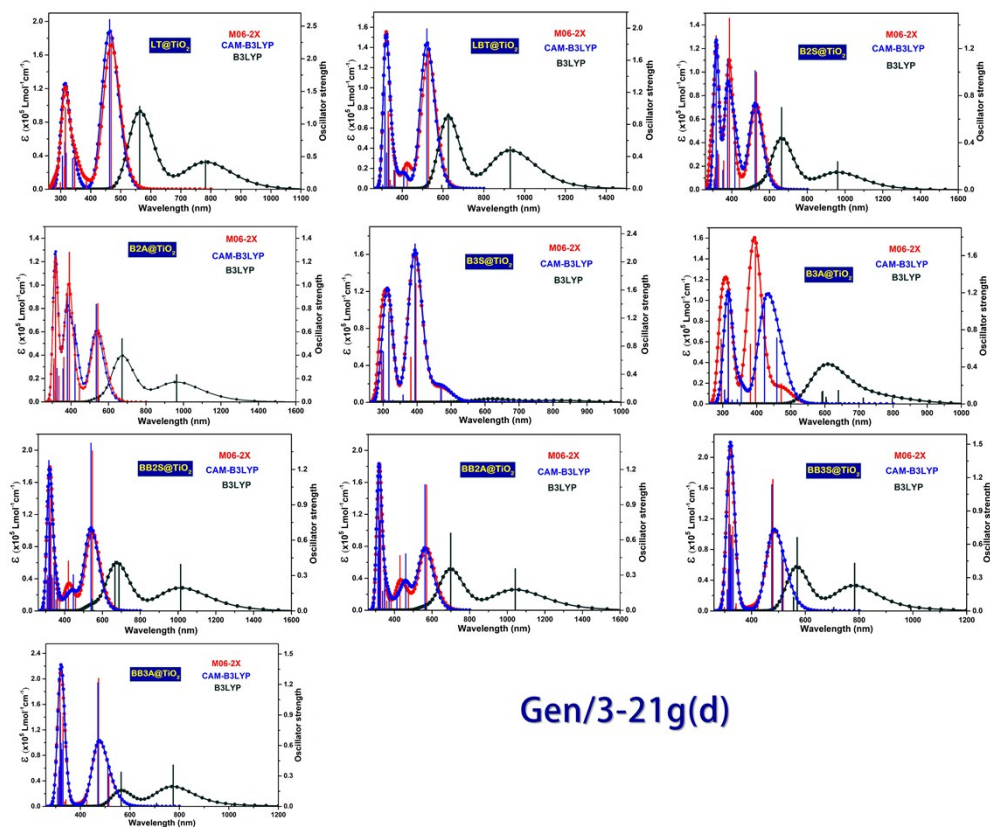
Fig. S21 Comparison of simulated absorption spectra of dyes@TiO$_2$ obtained from various functionals such as B3LYP, CAM-B3LYP and M062X/3-21g(d))/CPCM(THF) level of theory.
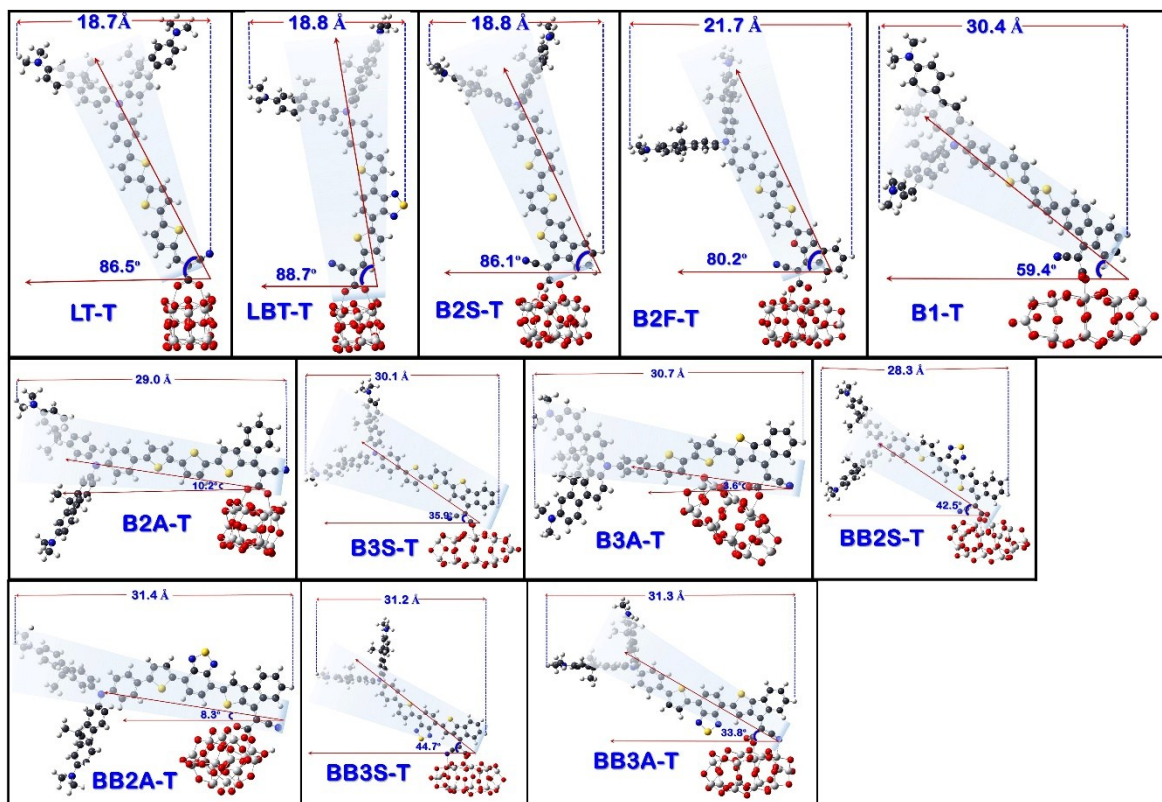
Fig. S22 Adsorption angle and the molecular coverage distance of the dyes@TiO₂.

Tables

Table S1: Computed S0- S1 excitation energies with electron volt in parenthesis, oscillator strength (f), major transitions and transient dipole moment of the dyes obtained from B3LYP/6-311g(d, p)/C-PCM(THF) level of theory.

BTD	λ$_{max}$ (nm)	f	Major transitions	μ$_e$ (D)
LT	848	0.42	HOMO->LUMO (99%)	19.55
	590	1.08	H-2->LUMO (96%)	
LBT	1002	0.53	HOMO->LUMO (100%)	19.39
	658	0.79	H-2->LUMO (84%), HOMO->L+1 (14%)	
B2	1086	0.28	HOMO->LUMO (100%)	18.29
	730	0.55	H-2->LUMO (93%), H-3->LUMO (4%)	
B3	555	1.03	HOMO->L+1 (96%), H-2->L+1 (2%)	12.29
	445	1.23	H-2->L+1 (89%), HOMO->L+1 (3%), HOMO->L+2 (3%)	
BB2	1125	0.4	HOMO->LUMO (100%)	12.37
	737	0.66	H-2->LUMO (63%), HOMO->L+1 (31%), H-3->LUMO (3%)	
BB3	799	0.46	HOMO->L+1 (98%)	17.35
	587	0.61	H-2->L+1 (91%), H-3->L+1 (2%)	

Table S2: Computed S0- S1 excitation energies with electron volt in parenthesis, oscillator strength (f), major transitions and transient dipole moment of the dyes obtained from CAM-B3LYP/6-311g(d, p)/C-PCM(THF) level of theory.

	λ_{max} (nm)	f	Major Transitions	μ_e (D)
LT	510	2.18	H-3->LUMO (13%), H-2->LUMO (46%), HOMO->LUMO (28%)	16.93
	357	0.52	H-2->L+1 (22%) HOMO->LUMO (25%) HOMO->L+1 (32%) HOMO->L+2 (10%)	
LBT	557	1.76	H-2->LUMO (43%) HOMO->LUMO (38%), H-3->LUMO (9%)	16.18
	426	0.14	H-3->L+1 (13%), H-2->L+1 (38%), HOMO->L+1 (23%)	
B2	591	0.76	H-4->LUMO (11%), H-3->LUMO (22%), H-2->LUMO (46%) HOMO->LUMO (14%)	15.56
	454	0.68	H-4->LUMO (20%), HOMO->LUMO (49%)	
B3	575	0.05	H-4->LUMO (16%), H-3->LUMO (25%), H-2->LUMO (45%)	11.25
	417	1.81	H-2->L+1 (34%), HOMO->LUMO (20%), HOMO->L+1 (27%)	
BB2	601	1.02	H-3->LUMO (18%), H-2->LUMO (46%), HOMO->LUMO (21%)	9.355
	491	0.54	H-4->LUMO (21%), H-3->LUMO (12%), H-2->L+1 (18%), HOMO->LUMO (23%), HOMO->L+1 (13%)	
BB3	537	0.63	H-3->LUMO (19%), H-2->LUMO (42%), HOMO->LUMO (13%)	16.03
	499	0.90	H-2->L+1 (44%), HOMO->L+1 (27%)	

Table S3. Bond length difference, hybridization, delocalization and stabilization energy of the dyes in the ground and excited state (in parenthesis) obtained from NBO analysis using B3LYP/6-311g(d, p) level of theory

| Dye	C_α-C_b[a] (Å)	C_b=C_v[a] (Å)	SP Hybridization[a]		Delocalization energy[a] (kcal/mol)	E2 (kcal/mol) [a] (X_β- C_α- C_b)		
			X_β- C_α	C_α- C_b		BD&CR	LP	Total
LT	1.421 (1.394)	1.368 (1.399)	3.48 (3.29)	1.72 (1.59)	4363.2 (4375.1)	17.98 (15.54)	2.95 (3.03)	20.93 (18.63)
LBT	1.422 (1.399)	1.367 (1.387)	3.44 (3.22)	1.59 (1.52)	53598.6 (53580.7)	18.04 (15.86)	3.02 (3.12)	21.06 (18.98)
B2	1.440 (1.441)	1.381 (1.422)	2.76 (2.79)	1.67 (1.64)	4854.8 (4855.9)	14.07 (13.41)	4.3 (4.3)	18.37 (17.71)
B3	1.476 (1.475)	1.374 (1.428)	2.19 (2.27)	2.03 (2.01)	4829.5 (4827.4)	13.88 (13.53)	-	13.88 (13.53)
BB2	1.447 (1.431)	1.380 (1.414)	2.72 (2.77)	1.68 (1.61)	54243.0 (54258.0)	14.17 (14.25)	4.5 (4.44)	18.67 (18.69)
BB3	1.474 (1.472)	1.365 (1.421)	2.21 (2.20)	2.04 (1.97)	54050.5 (54070.1)	17.98 (17.53)	-	17.98 (17.53)
B2F	1.431 (1.431)	1.384 (1.420)	2.99 (2.99)	1.59 (1.59)	4841.9 (4843.8)	13.91 (13.17)	6.07 (6.15)	19.98 (19.32)
B1	1.486 (1.467)	1.363 (1.420)	2.23 (2.27)	2.23 (2.10)	4911.4 (4926.9)	13.31 (13.25)	-	13.31 (13.25)

[a]values obtained from B3LYP/6-311G(d, p) level of theory. [b]stabilization energy obtained from second order theory analysis.

Table S4: C_{AO} of the valence orbitals of X_β-C_α-C_b-C_v involved and their population in the ground state and excited state (in parenthesis) respectively.
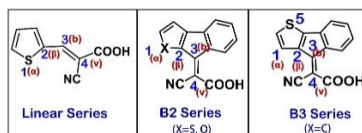
		S	Px	Py	Pz
LT	**S (1)**	0.75648 (0.75641)	-0.00645 (-0.00794)	0.09345 (0.25209)	0.26363 (0.08696)
	C (2)	0.44453 (0.44261)	0.19709 (0.21495)	0.23107 (0.48125)	0.44126 (0.25531)
	C (3)	0.34684 (0.36914)	0.09755 (0.08618)	0.24230 (0.30690)	0.31138 (0.22801)
	C (4)	0.33169 (0.33220)	0.23809 (0.21675)	0.19396 (0.42546)	0.42743 (0.22495)
LBT	**S (1)**	0.75256 (0.75145)	0.00256 (0.00637)	0.07421 (0.18753)	0.27070 (0.12804)
	C (2)	0.44644 (0.44235)	0.19352 (0.18143)	0.23112 (0.36945)	0.43992 (0.32177)
	C (3)	0.35033 (0.37285)	0.15141 (0.15297)	0.19035 (0.25389)	0.31199 (0.20619)
	C (4)	0.33230 (0.33342)	0.23446 (0.20200)	0.19739 (0.35291)	0.42709 (0.30709)
B2	**S (1)**	0.74187 (-0.01153)	-0.01503 (-0.01153)	0.15418 (0.24005)	0.17593 (0.09313)
	C (2)	0.41911 (0.42526)	0.14871 (0.15459)	0.31051 (0.43645)	0.36347 (0.23685)
	C (3)	0.32562 (0.32101)	0.15042 (0.14891)	0.26582 (0.31276)	0.27446 (0.23924)
	C (4)	0.27315 (0.28030)	0.17130 (0.17211)	0.32054 (0.41046)	0.36214 (0.25244)
B3	**S (5)**	0.74825 (0.74766)	0.00856 (0.00840)	0.10197 (0.12681)	0.24581 (0.22110)
	C (1)	0.34869 (0.34488)	0.17880 (0.18580)	0.15322 (0.15763)	0.32045 (0.32045)
	C (2)	0.33392 (0.34195)	0.19179 (0.19487)	0.19048 (0.21636)	0.36714 (0.32899)
	C (3)	0.31093 (0.30069)	0.21953 (0.21136)	0.19118 (0.20355)	0.29853 (0.25821)
	C (4)	0.26161 (0.27943)	0.15134 (0.15943)	0.28518 (0.30490)	0.40727 (0.35385)
BB2	**S (1)**	0.73405 (0.73397)	-0.00173 (-0.0080)	0.07107 (0.17589)	0.26205 (0.13711)
	C (2)	0.41719 (0.41925)	0.11505 (0.12079)	0.24355 (0.36452)	0.44965 (0.32883)
	C (3)	0.33545 (0.33348)	0.21506 (0.21423)	0.17745 (0.25141)	0.30485 (0.22463)
	C (4)	0.32793 (0.32553)	0.11498 (0.10584)	0.24749 (0.35060)	0.42109 (0.31829)
BB3	**S (5)**	0.74143 (0.74473)	0.01665 (0.01975)	0.15443 (0.25833)	0.18645 (0.07825)
	C (1)	0.34602 (0.34675)	0.10458 (0.10706)	0.22744 (0.23625)	0.26848 (0.15222)
	C (2)	0.33691 (0.34131)	0.20651 (0.19895)	0.26142(0.29661)	0.28112 (0.17318)
	C (3)	0.30260 (0.30026)	0.15765 (0.19283)	0.24071 (0.25234)	0.28452 (0.17605)
	C (4)	0.28453 (0.30489)	0.17056 (0.17471)	0.29225 (0.38994)	0.33380 (0.21631)
B2F	**O (1)**	0.82359 (0.82738)	0.36415 (0.36533)	0.50011 (0.57881)	0.55080 (0.47861)
	C (2)	0.39801 (0.39914)	-0.00394 (-0.00404)	0.15158 (0.35682)	0.29714(0.08878)
	C (3)	0.29148 (0.28987)	0.20994 (0.21151)	0.19804 (0.31019)	0.26811 (0.15244)
	C (4)	0.24673 (0.25259)	0.14610 (0.13390)	0.31626 (0.42367)	0.39332 (0.27649)
B1	**C (1)**	0.33962 (0.36547)	0.14098 (0.12666)	0.25328 (0.25744)	0.28627 (0.27667)
	C (2)	0.32964 (0.32922)	0.16036 (0.15846)	0.25608 (0.24682)	0.33753(0.33709)
	C (3)	0.31407 (0.31193)	0.21293 (0.21412)	0.21175 (0.20931)	0.25963 (0.27168)
	C (4)	0.28747 (0.30904)	0.17460 (0.21532)	0.25765 (0.24756)	0.36175 (0.32047)

Table S5: Hybridization state of the atoms involving in resonance interactions from the contribution of the corresponding bonds (X_β-C_α-C_b-C_v).
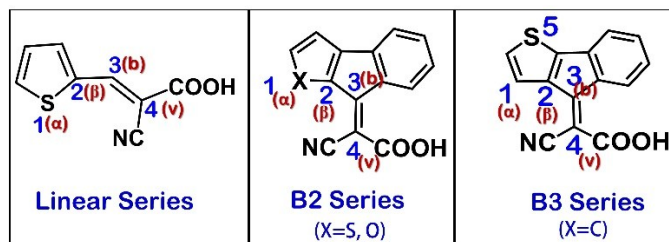
	Bond	Atom	Ground state	Hybrid	Excited state	
LT	S_β-C_α	S_β	s(19.11%), p (80.34%)	sp$^{4.20}$	s (18.48%), p (81.38%)	sp$^{4.38}$
		C_α	s (22.29%), p (77.52%)	sp$^{3.48}$	s (23.26%), p (46.56%)	sp$^{3.29}$
	C_α-C_b	C_α	s (36.81%), p (63.15%)	sp$^{1.72}$	s (37.60%), p (62.36%)	sp$^{1.59}$
		C_b	s (38.61%), p (61.35%)	sp$^{1.59}$	s (39.62%), p (60.34%)	sp$^{1.52}$
	C_b-C_v	C_b	s (37.63%), p (62.34%)	sp$^{1.66}$	s (36.60%), p (63.36%)	sp$^{1.73}$
		C_v	s (38.33%), p (61.64%)	sp$^{1.61}$	s (37.15%), p (62.82%)	sp$^{1.69}$
LBT	S_β-C_α	S_β	s (19.32%), p (80.13%)	sp$^{4.15}$	s (18.82%), p (80.65%)	sp$^{4.29}$
		C_α	s (22.45%), p (77.35%)	sp$^{3.44}$	s (23.67%), p (76.15%)	sp$^{3.22}$
	C_α-C_b	C_α	s (38.61%), p (61.35%)	sp$^{1.59}$	s (39.62%), p (60.34%)	sp$^{1.52}$
		C_b	s (38.37%), p (61.59%)	sp$^{1.61}$	s (39.12%), p (60.84%)	sp$^{1.56}$
	C_b-C_v	C_b	s (37.62%), p (62.34%)	sp$^{1.66}$	s (36.97%), p (62.99%)	sp$^{1.70}$
		C_v	s (38.41%), p (61.56%)	sp$^{1.60}$	s (37.67%), p (62.30%)	sp$^{1.65}$
B2	S_β-C_α	S_β	s (19.57%), p (79.87%)	sp$^{4.08}$	s (21.32%), p (78.64%)	sp$^{3.67}$
		C_α	s (26.56%), p (73.28%)	sp$^{2.76}$	s (26.34%), p (73.50%)	sp$^{2.79}$
	C_α-C_b	C_α	s(37.48%), p (62.48%)	sp$^{1.67}$	s (37.93%), p (62.03%)	sp$^{1.64}$
		C_b	s (30.63%), p (69.32%)	sp$^{2.26}$	s (30.78%), p (69.18%)	sp$^{2.25}$
	C_b-C_v	C_b	s (37.27%), p (62.69%)	sp$^{1.68}$	s (36.11%), p (63.86%)	sp$^{1.77}$
		C_v	s (39.43%), p (60.52%)	sp$^{1.53}$	s (37.92%), p (62.06%)	sp$^{1.64}$
B3	C_β-C_α	C_β	s (35.89%), p (64.07%)	sp$^{1.79}$	s(35.23%), p (64.73%)	sp$^{1.84}$
		C_α	s (31.30%), p (68.66%)	sp$^{2.19}$	s (30.53%), p (69.43%)	sp$^{2.27}$
	C_α-C_b	C_α	s(33.03%), p (66.93%)	sp$^{2.03}$	s (34.16%), p (65.80%)	sp$^{2.01}$
		C_b	s (30.28%), p (69.67%)	sp$^{2.30}$	s (30.82%), p (69.13%)	sp$^{2.26}$
	C_b-C_v	C_b	s (37.35%), p (62.61%)	sp$^{1.68}$	s (35.73%), p (64.24%)	sp$^{1.80}$
		C_v	s (40.10%), p (59.87%)	sp$^{1.49}$	s (37.75%), p (62.22%)	sp$^{1.65}$
BB2	S_β-C_α	S_β	s (21.68%), p (78.28%)	sp$^{3.61}$	s (21.55%), p (78.05%)	sp$^{3.63}$
		C_α	s (26.87%), p (72.98%)	sp$^{2.72}$	s (26.48%), p (73.36%)	sp$^{2.77}$
	C_α-C_b	C_α	s(37.26%), p (62.71%)	sp$^{1.68}$	s (38.26%), p (61.70%)	sp$^{1.61}$
		C_b	s (30.60%), p (69.35%)	sp$^{2.27}$	s (31.49%), p (68.47%)	sp$^{2.17}$
	C_b-C_v	C_b	s (37.35%), p (62.62%)	sp$^{1.68}$	s (36.35%), p (63.61%)	sp$^{1.75}$
		C_v	s (39.04%), p (60.93%)	sp$^{1.56}$	s (37.83%), p (62.15%)	sp$^{1.64}$
BB3	C_β-C_α	C_β	s(35.82%), p (64.13%)	sp$^{1.79}$	s (35.44%), p (64.52%)	sp$^{1.82}$
		C_α	s (31.11%), p (68.85%)	sp$^{2.21}$	s (33.56%), p (66.40%)	sp$^{2.20}$
	C_α-C_b	C_α	s(32.93%), p (67.03%)	sp$^{2.04}$	s (34.04%), p (65.92%)	sp$^{2.01}$
		C_b	s (31.39%), p (68.57%)	sp$^{2.18}$	s (31.70%), p (68.25%)	Sp$^{2.15}$
	C_b-C_v	C_b	s (37.40%), p (62.57%)	sp$^{1.67}$	s (35.81%), p (64.16%)	sp$^{1.79}$
		C_v	s (40.24%), p (59.73%)	sp$^{1.48}$	s (37.45%), p (62.52%)	sp$^{1.67}$
B2F	O_β-C_α	O_β	s (32.5%), p (67.32%)	sp$^{2.07}$	s (32.66%), p (67.27%)	sp$^{2.06}$
		C_α	s (25.03%), p (74.33%)	sp$^{2.99}$	s (25.02%), p (74.75%)	sp$^{2.99}$
	C_α-C_b	C_α	s(38.55%), p (61.42%)	sp$^{1.59}$	s (38.63%), p (61.34%)	sp$^{1.59}$
		C_b	s (29.83%), p (70.11%)	sp$^{2.35}$	s (29.64%), p (70.30%)	sp$^{2.37}$
	C_b-C_v	C_b	s (38.09%), p (61.87%)	sp$^{1.62}$	s (36.95%), p (63.03%)	sp$^{1.71}$
		C_v	s (39.07%), p (60.90%)	sp$^{1.56}$	s (37.64%), p (62.33%)	sp$^{1.66}$
B1	C_β-C_α	C_β	s (35.93%), p (64.03%)	sp$^{2.18}$	s (35.27%), p (64.68%)	sp$^{1.83}$
		C_α	s (36.89%), p (63.08%)	sp$^{2.23}$	s (36.11%), p (63.86%)	sp$^{2.27}$
	C_α-C_b	C_α	s(30.90%), p (69.06%)	sp$^{2.23}$	s (32.23%), p (67.73%)	sp$^{2.10}$
		C_b	s (31.42%), p (68.54%)	sp$^{2.18}$	s (32.01%), p (67.95%)	sp$^{2.12}$
	C_b-C_v	C_b	s (37.28%), p (62.69%)	sp$^{1.68}$	s (35.71%), p (64.26%)	sp$^{1.80}$
		C_v	s (40.90%), p (59.47%)	sp$^{1.47}$	s (37.67%), p (62.30%)	sp$^{1.65}$

(X_β: Heteroatoms at β- substitution; C_α: carbon; C_b: bridging carbon; C_v: vinylenic carbon).

Table S6. Energy Levels, computed excitation energies, oscillator strength, major electronic transitions, ground and transient dipole moment of the dyes@TiO$_2$

	HOMO[a] (eV)	LUMO[a] (eV)	HL Gap[a] (eV)	λ_{max}[b] (nm)	f	Major compositions	μ_g (Debye)	μ_e (Debye)
LT-T	-4.71	-3.92	0.79	525.9 (2.36)	2.40	H->L (84%), H-2->L (9%), H-2->L+1 (7%)	18.9	21.0
LBT-T	-4.74	-3.94	0.80	577.1 (2.15)	1.84	H->L (89%), H-2->L (7%), H-3->L (4%)	20.9	23.8
B2S-T	-4.64	-3.99	0.65	603.1 (2.06)	0.96	H->L (59%), H-3->L (16%), H-2->L (21%), H-4->L (3%)	16	18.2
B2A-T	-4.62	-3.95	0.67	578.9 (2.14)	0.82	H->L (61%), H-3->L (17%), H-2->L (19%), H-4->L (3%)	12.6	14.8
B3S-T	-4.63	-3.92	0.71	493.1 (2.51)	0.17	H-3->L+2 (11%), H-2->L+2 (29%), H-2->L+3 (17%), H-4->L+2 (5%), H-4->L+3 (3%), H-3->L+1 (2%), H-3->L+3 (7%), H-2->L+1 (5%), H->L+2 (8%), H->L+3 (4%)	15.0	16.4
B3A-T	-4.73	-3.79	0.94	488.0 (2.54)	0.09	H->L (10%), H-3->L+1 (13%), H-2->L (11%), H-4->L+1 (5%), H-3->L (2%), H-2->L+4 (2%), H-2->L+9 (2%), H->L+1 (8%), H->L+9 (2%)	19.7	23.2
BB2S-T	-4.72	-3.81	0.91	617.3 (2.01)	1.36	H->L (67%), H-2->L (22%), H-3->L (9%)	18.6	19.9
BB2A-T	-4.64	-3.96	0.68	605.5 (2.07)	1.02	H->L (62%), H-3->L (13%), H-2->L (15%)	10.7	12.5
BB3S-T	-4.67	-3.71	0.96	540.9 (2.29)	0.32	H->L (45%), H-3->L (15%), H-2->L (17%), H-4->L (6%), H-2->L+2 (7%)	19.6	21.2
BB3A-T	-4.61	-3.73	0.88	538.7 (2.30)	0.26	H->L (43%), H-3->L (18%), H-2->L (21%), H-4->L (8%), H-2->L+2 (9%)	16.4	18.9
B2F-T	-4.64	-3.98	0.66	609.2 (2.04)	0.90	HOMO->LUMO (53%), H-3->LUMO (15%), H-2->LUMO (18%), H-4->LUMO (6%)	16.3	19.1
B1-T	-4.54	-4.13	0.41	457.8 (2.71)	0.40	H-3->L+2 (10%), H-2->L+2 (27%), HOMO->L+2 (16%), H-4->L+1 (2%), H-4->L+2 (6%), H-3->L+1 (4%), H-2->L+1 (9%), H-2->L+4 (3%), HOMO->L+1 (6%)	11.9	13.7

[a]values obtained from B3LYP/6-311g(d,p). [b]values obtained from M06-2X/6-311g(d,p)/C-PCM(THF) and electron volt values are given in parenthesis. [c]ground state (μ_g) and excited state (μ_g) dipole moments computed from B3LYP/6-311g(d, p) level of theory.

Table S7: Computed S0- S1 excitation energies with electron volt in parenthesis, oscillator strength (f), major transitions and transient dipole moment of the dyes@TiO$_2$ obtained from B3LYP/6-311g(d, p)/C-PCM(THF) level of theory.

BTD	λ_{max} (nm)	f	Major transitions	μ_e (D)
LT-T	822.3 (1.51)	0.43	HOMO->L+2 (16%), HOMO->L+3 (81%)	21.0
	808.3 (1.53)	0.03	HOMO->L+2 (84%), HOMO->L+3 (16%)	
LBT-T	966.6 (1.28)	0.58	HOMO->LUMO (99%)	23.8
	659.9 (1.88)	0.29	H-2->LUMO (22%), HOMO->L+11 (60%), HOMO->L+13 (11%)	
B2S-T	986.1 (1.26)	0.29	HOMO->LUMO (99%)	18.2
	699.1 (1.77)	0.66	H-2->LUMO (90%), H-3->LUMO (5%)	
B2A-T	996.8 (1.24)	0.27	HOMO->LUMO (99%)	14.8
	707.2 (1.75)	0.48	H-2->LUMO (90%), H-3->LUMO (5%)	
B3S-T	814.1 (1.52)	0.01	HOMO->L+3 (67%), HOMO->L+4 (13%), HOMO->L+5 (13%)	16.4
	803.2 (1.54)	0.01	HOMO->L+3 (31%), HOMO->L+4 (37%), HOMO->L+5 (23%)	
B3A-T	980.3 (1.27)	0.02	HOMO->LUMO (97%)	23.2
	704.7 (1.76)	0.06	H-2->LUMO (13%), H-1->LUMO (34%), HOMO->L+10 (43%)	
BB2S-T	1009.8 (1.28)	0.47	HOMO->LUMO (99%)	19.9
	707.2 (1.75)	0.27	H-2->LUMO (10%), HOMO->L+11 (77%)	

	1074.7 (1.15)	0.39	HOMO->LUMO (99%)	
BB2A-T				12.5
	730.0 (1.70)	0.46	H-2->LUMO (52%), HOMO->L+9 (16%), HOMO->L+11 (21%)	
BB3S-T	815.1 (1.52)	0.27	HOMO->L+4 (61%), HOMO->L+6 (26%)	21.2
	790.6 (1.57)	0.18	HOMO->L+4 (34%), HOMO->L+6 (54%)	
BB3A-T	783.9 (1.58)	0.30	HOMO->L+6 (36%), HOMO->L+8 (41%)	18.9
	756.9 (1.64)	0.03	HOMO->L+6 (52%), HOMO->L+7 (24%), HOMO->L+8 (21%)	

Table S8: Computed S0- S1 excitation energies with electron volt in parenthesis, oscillator strength (f), major transitions and transient dipole moment of the dyes@TiO$_2$ obtained from CAM-B3LYP/6-311g (d, p)/C-PCM(THF) level of theory.

CTD	λ_{max} (nm)	f	Major transitions	μ_e (D)
LT-T	514.9 (2.41)	2.56	HOMO->LUMO (68%), H-3->LUMO (13%), H-2->LUMO (9%), H-2->L+1 (5%), HOMO->L+1 (5%)	18.7
	355.2(3.49)	0.39	HOMO->LUMO (20%), H-2->L+25 (12%), HOMO->L+1 (19%), HOMO->L+25 (15%)	
LBT-T	568.1 (2.18)	1.94	HOMO->LUMO (78%), H-2->LUMO (13%), H-3->LUMO (7%), HOMO->L+1 (2%)	21.0
	330.8 (2.95)	1.18	HOMO->L+44 (77%) H-1->L+51 (6%)	
B2S-T	594.0 (2.09)	0.96	HOMO->LUMO (52%), H-3->LUMO (29%), H-2->LUMO (11%),	16.2
	432.0 (2.87)	0.97	HOMO->LUMO (38%), H-4->LUMO (18%), HOMO->L+22 (10%)	
B2A-T	572.2(2.17)	0.80	HOMO->LUMO (54%), H-3->LUMO (21%), H-2->LUMO (25%),	12.9
	438.1(2.83)	0.91	HOMO->LUMO (38%), H-4->LUMO (19%), H->L+3 (33%)	
B3S-T	490.4 (2.53)	0.20	H-3->L+3 (15%), H-2->L+2 (13%), H-2->L+3 (34%), H-4->L+3 (8%), H-3->L+2 (6%), HOMO->L+3 (6%)	16.4
	414.8 (2.99)	2.30	H-2->L+19 (31%), HOMO->L+19 (24%), H-2->L+17 (4%), H-2->L+18 (4%), H-2->L+20 (4%), HOMO->L+20 (4%), HOMO->L+39 (5%)	
B3A-T	485.6 (2.55)	0.13	HOMO->LUMO (5%), H-3->L+2 (17%), H-2->L+2 (29%), H-4->L+2 (7%), H-2->LUMO (9%), HOMO->L+2 (7%)	22.1
	458.0 (2.71)	0.67	HOMO->LUMO (10%), H-4->L+2 (5%), H-3->L+2 (7%), H-2->LUMO (7%), H-2->L+2 (7%), H-2->L+4 (5%), H-2->L+5 (6%), H-2->L+9 (5%), H-2->L+15 (4%), HOMO->L+5 (5%)	
BB2S-T	606.9 (2.04)	1.39	HOMO->LUMO (66%), H-3->LUMO (13%), H-2->LUMO (18%),	17.4
	466.1(2.66)	0.35	HOMO->LUMO (14%), H-4->LUMO (19%), H-3->LUMO (16%), H-2->L+7 (11%)	
BB2A-T	598.1(2.07)	1.01	HOMO->LUMO (62%), H-3->LUMO (16%), H-2->LUMO (19%)	10.3
	484.9 (2.56)	0.55	HOMO->LUMO (18%), H-4->LUMO (20%), H-3->LUMO (13%), H-2->L+7 (10%)	
BB3S-T	536.2(2.31)	0.41	HOMO->LUMO (69%), H-3->LUMO (15%), H-2->LUMO (3%), H-2->L+1 (12%)	20.0
	504.1 (2.46)	1.02	H-2->L+3 (20%), HOMO->L+3 (11%), H-4->LUMO (5%), H-3->LUMO (6%), H-2->LUMO (5%), H-2->L+1 (7%), H-2->L+4 (9%), H-2->L+5 (5%), HOMO->L+1 (6%)	
BB3A-T	533.0 (2.33)	0.29	HOMO->LUMO (68%), H-3->LUMO (16%), H-2->LUMO (8%), H-4->LUMO (8%)	17.9
	497.5 (2.49)	1.19	H-2->L+4 (35%), HOMO->L+4 (19%), H-4->LUMO (4%), H-3->L+4 (3%), H-2->L+5 (9%)	

Table S9: Computed S0- S1 excitation energies with electron volt in parenthesis, oscillator strength (f), major transitions and transient dipole moment of the dyes@TiO_2 obtained from B3LYP/3-21g(d)/C-PCM(THF) level of theory.

BTD	λ_{max} (nm)	f	Major transitions	μ_e (D)
LT	782.4 (1.58)	0.44	HOMO->LUMO (99%	20.4
	563.3 (2.17)	1.27	H-2->LUMO (95%)	
LBT	929.6 (1.33)	0.52	HOMO->LUMO (99%)	22.9
	626.2 (1.98)	0.94	H-2->LUMO (90%), HOMO->L+5 (5%)	
B2S-T	961.3 (1.29)	0.24	HOMO->LUMO (99%)	18.2
	664.2 (1.87)	0.69	H-2->LUMO (92%), H-3->LUMO (5%)	
B2A-T	963.6 (1.29)	0.23	HOMO->LUMO (99%	13.9
	672.2 (1.84)	0.54	H-2->LUMO (93%), H-3->LUMO (5%)	
B3S-T	817.9 (1.52)	0.03	HOMO->LUMO (98%)	16.8
	629.4 (1.97)	0.05	H-3->LUMO (11%), H-2->LUMO (84%), HOMO->LUMO (2%)	
B3A-T	797.4 (1.55)	0.06	HOMO->LUMO (98%)	22.7
	639.4 (1.94)	0.15	HOMO->L+4 (93%), HOMO->L+5 (3%)	
BB2S-T	1013. (1.22)	0.39	HOMO->LUMO (99%)	19.9
	687.7 (1.80)	0.40	H-2->LUMO (16%), HOMO->L+1 (13%), HOMO->L+2 (66%)	
BB2A-T	1042.4 (1.19)	0.36	HOMO->LUMO (99%)	12.0
	699.0 (1.77)	0.66	H-2->LUMO (72%), HOMO->L+1 (12%), HOMO->L+2 (9%)	
BB3S-T	992.4 (1.25)	0.03	HOMO->LUMO (99%)	21.0
	783.3 (1.58)	0.43	HOMO->L+1 (99%)	
BB3A-T	1010.7 (1.23)	0.02	HOMO->LUMO (99%)	19.0
	775.0 (1.59)	0.41	HOMO->L+1 (98%)	

Table S10: Computed S0- S1 excitation energies with electron volt in parenthesis, oscillator strength (f), major transitions and transient dipole moment of the dyes@TiO_2 obtained from CAM-B3LYP/3-21g(d)/C-PCM(THF) level of theory.

CTD	λ_{max} (nm)	f	Major transitions	μ_e (D)
LT	462.8 (2.68)	2.60	H-3->LUMO (8%), H-2->LUMO (15%), HOMO->LUMO (76%)	18.3
	339.8 (3.65)	0.47	H-2->L+16 (11%), HOMO->LUMO (26%), HOMO->L+16 (15%)	
LBT	521.0 (2.38)	1.99	H-3->LUMO (2%), H-2->LUMO (18%), HOMO->LUMO (78%)	20.4
	334.3 (3.71)	0.75	H-3->LUMO (12%), H-2->L+26 (13%), HOMO->L+26 (30%),	
B2S-T	523.7 (2.37)	1.01	H-3->LUMO (13%), H-2->LUMO (15%), HOMO->LUMO (62%), H-4->LUMO (9%)	16.1

	λmax (nm)	f	Major transitions	μe (D)
	378.0 (3.28)	1.10	H-5->LUMO (10%), H-4->LUMO (10%), H-2->LUMO (11%), HOMO->LUMO (34%)	
B2A-T	534.6 (2.32)	0.83	H-3->LUMO (14%), H-2->LUMO (16%), HOMO->LUMO (63%), H-4->LUMO (7%)	12.1
	420.9 (2.95)	0.66	H-4->LUMO (17%), HOMO->LUMO (49%), H-5->LUMO (6%), H-3->LUMO (9%)	
B3S-T	469.7 (2.64)	0.25	H-4->LUMO (12%), H-3->LUMO (27%), H-2->LUMO (46%), HOMO->LUMO (9%)	15.9
	393.9 (3.15)	2.25	H-2->L+11 (30%), HOMO->L+11 (25%) H-4->LUMO (3%), H-3->L+32 (2%), H-2->L+12 (9%), HOMO->LUMO (3%), HOMO->L+12 (8%), HOMO->L+32 (6%)	
B3A-T	458.9 (2.70)	0.71	H-3->LUMO (27%), H-2->LUMO (38%), HOMO->LUMO (11%), H-4->LUMO (9%)	21.6
	422.9 (2.93)	1.14	H-2->L+1 (18%), HOMO->L+1 (14%), H-4->LUMO (7%), H-3->LUMO (7%), H-3->L+1 (3%), H-2->L+2 (5%), H-2->L+3 (9%), H-2->L+6 (2%), H-2->L+7 (3%), HOMO->L+2 (4%), HOMO->L+3 (7%), HOMO->L+7 (2%)	
BB2S-T	539.2 (2.29)	1.42	H-3->LUMO (9%), H-2->LUMO (34%), HOMO->LUMO (57%)	17.4
	445.9 (2.78)	0.30	H-4->LUMO (20%), H-3->LUMO (17%), H-2->L+1 (13%), HOMO->LUMO (22%), HOMO->L+1 (11%)	
BB2A-T	562.4 (2.20)	1.01	H-3->LUMO (16%), H-2->LUMO (31), HOMO->LUMO (52%)	10.0
	484.9 (2.69)	0.55	H-4->LUMO (20%), H-3->LUMO (13%), H-2->L+7 (10%), HOMO->LUMO (18%)	
BB3S-T	513.2 (2.42)	0.56	H-3->LUMO (22%), H-2->LUMO (42%), HOMO->LUMO (32%), H-4->LUMO (6%)	19.8
	475.5 (2.60)	1.14	H-2->L+1 (45%), HOMO->L+1 (27%), H-4->LUMO (6%), H-3->L+1 (7%)	
BB3A-T	510.9 (2.43)	0.42	H-4->LUMO (5%), H-3->LUMO (12%), H-2->LUMO (43%), HOMO->LUMO (40%)	18.0
	470.8 (2.63)	1.21	H-2->L+1 (47%), HOMO->L+1 (28%), H-4->LUMO (5%), H-3->L+1 (6%)	

Table S11: Computed S0- S1 excitation energies with electron volt in parenthesis, oscillator strength (f), major transitions and transient dipole moment of the dyes@TiO$_2$ obtained from M062X/3-21g(d)/C-PCM(THF) level of theory.

MTD	λmax (nm)	f	Major transitions	μe (D)
LT	468.1 (2.65)	2.38	H-3->LUMO (10%), H-2->LUMO (12%), HOMO->LUMO (77%)	18.5
	315.6 (3.21)	1.25	HOMO->L+32 (80%), H-1->L+34 (4%), H-1->L+50 (3%)	
LBT	528.4 (2.35)	1.82	H-2->LUMO (13%), HOMO->LUMO (81%), H-3->LUMO (6%)	20.6
	424.9 (2.92)	0.33	H-3->LUMO (20%), H-2->LUMO (34%), HOMO->LUMO (42%)	
B2S-T	530.7 (2.33)	0.99	H-3->LUMO (8%), H-2->LUMO (29%), HOMO->LUMO (60%), H-4->LUMO (3%)	16.3
	387.3 (2.82)	1.46	H-5->LUMO (10%), H-4->LUMO (20%), H-2->LUMO (14%), H-2->L+6 (12%), HOMO->LUMO (10%), H-6->LUMO (2%), H-2->L+5 (6%), HOMO->L+5 (5%), HOMO->L+6 (9%)	
B2A-T	542.5 (2.29)	0.84	H-3->LUMO (16%), H-2->LUMO (28%), HOMO->LUMO (55%)	12.2
	390.8 (2.79)	1.28	H-5->LUMO (13%), H-4->LUMO (20%), H-2->LUMO (16%), H-2->L+6 (12%), HOMO->LUMO (11%)	
B3S-T	471.4(2.63)	0.22	H-3->LUMO (23%), H-2->LUMO (49%), HOMO->LUMO (14%), H-4->LUMO (9%)	16.2
	396.3 (3.13)	1.69	H-2->L+3 (26%), HOMO->LUMO (20%), HOMO->L+3 (31%)	
B3A-T	488.0 (2.54)	0.63	H-3->LUMO (23%), H-2->LUMO (40%), HOMO->LUMO (17%)	22.1
	424.2 (2.66)	1.20	H-2->L+1 (32%), HOMO->L+1 (36%), H-4->LUMO (6%), H-3->LUMO (7%)	

BB2S-T	546.5 (2.27)	1.35	H-3->LUMO (10%), H-2->LUMO (29%), HOMO->LUMO (61%)	17.8
	327.1(2.71)	1.02	H-2->L+19 (14%), HOMO->L+19 (55%)	
BB2A-T	570.5(2.17)	1.06	H-3->LUMO (13%), H-2->LUMO (23%), HOMO->LUMO (64%)	10.1
	474.2(2.61)	0.20	H-4->LUMO (13%), H-3->LUMO (19%), HOMO->LUMO (41%), H-2->LUMO (9%)	
BB3S-T	516.9(2.39)	0.45	H-3->LUMO (19%), H-2->LUMO (13%), HOMO->LUMO (58%), H-4->LUMO (8%)	19.9
	479.3(2.59)	1.18	H-2->L+1 (40%), HOMO->L+1 (38%), H-4->LUMO (5%), H-3->LUMO (5%)	
BB3A-T	515.2(2.41)	0.32	H-3->LUMO (19%), H-2->LUMO (15%), HOMO->LUMO (57%), H-4->LUMO (9%)	18.1
	473.6 (2.62)	1.26	H-2->L+1 (42%), HOMO->L+1 (39%), H-4->LUMO (4%), H-3->L+1 (4%)	

References

1. Gaussian 09, Revision B.01, M. J. Frisch, G. W. Trucks, H. B. Schlegel, G. E. Scuseria, M. A. Robb, J. R. Cheeseman, G. Scalmani, V. Barone, G. A. Petersson, H. Nakatsuji, X. Li, M. Caricato, A. Marenich, J. Bloino, B. G. Janesko, R. Gomperts, B. Mennucci, H. P. Hratchian, J. V. Ortiz, A. F. Izmaylov, J. L. Sonnenberg, D. Williams-Young, F. Ding, F. Lipparini, F. Egidi, J. Goings, B. Peng, A. Petrone, T. Henderson, D. Ranasinghe, V. G. Zakrzewski, J. Gao, N. Rega, G. Zheng, W. Liang, M. Hada, M. Ehara, K. Toyota, R. Fukuda, J. Hasegawa, M. Ishida, T. Nakajima, Y. Honda, O. Kitao, H. Nakai, T. Vreven, K. Throssell, J. A. Montgomery, Jr., J. E. Peralta, F. Ogliaro, M. Bearpark, J. J. Heyd, E. Brothers, K. N. Kudin, V. N. Staroverov, T. Keith, R. Kobayashi, J. Normand, K. Raghavachari, A. Rendell, J. C. Burant, S. S. Iyengar, J. Tomasi, M. Cossi, J. M. Millam, M. Klene, C. Adamo, R. Cammi, J. W. Ochterski, R. L. Martin, K. Morokuma, O. Farkas, J. B. Foresman, and D. J. Fox, Gaussian, Inc., Wallingford CT, **2010**.

2. A. Leliège, J. Grolleau, M. Allain, P. Blanchard, D. Demeter, T. Rousseau and J. Roncali, *Chem. Eur. J.*, 2013, **19**, 9948-9960.

3. D. Demeter, F. Melchiorre, P. Biagini, R. Po and J. Roncali, *Tetrahedron Lett.*, 2016, **57**, 505-508.

4. Z. Wang, A. Putta, J. D. Mottishaw, Q. Wei, H. Wang and H. Sun, *J. Phys. Chem. C*, 2013, **117**, 16759-16768.

5. J. Shi, W. Zhao, L. Xu, Y. Kan, C. Li, J. Song and H. Wang, *J. Phys. Chem. C*, 2014, **118**, 7844-7855.